The Route to Spring Phytoplankton Blooms Simulated by a Lagrangian Plankton Model

Yign Noh[1], Kyung Min Noh[2], Ashley Brereton[1], and Jong-Seong Kug[2]

[1]Yonsei University
[2]POSTECH

November 26, 2022

Abstract

A Lagrangian plankton model (LPM) is developed, in which the motion of a large number of Lagrangian particles, representing a plankton community, is calculated under the turbulence field simulated by large eddy simulation. A spring phytoplankton bloom is realized using the LPM, and the mechanism for its generation is investigated. Mixing by convective eddies during the night helps to maintain the uniform concentration of phytoplankton within the mixed layer, even if the daily mean surface heat flux is positive in spring. Accordingly, the spring bloom can be predicted by the critical depth hypothesis, if the mixing layer is used instead of the mixed layer. The shoaling of the mixing layer occurs immediately after the start of surface heating, but the shoaling of the mixed layer is delayed. A new criterion for the spring bloom is proposed, which predicts that spring blooms are more likely to occur at higher latitudes, even if the atmospheric forcing is the same. Furthermore, various statistics of Lagrangian particles, such as the vertical migration of plankton, the residence time of plankton within the euphotic zone, and the growth of plankton are investigated by taking advantage of the LPM.

The Route to Spring Phytoplankton Blooms Simulated by a Lagrangian Plankton Model

Kyung Min Noh[1], Yign Noh*[2], Ashley Brereton[2], and Jong-Seong Kug[1]

1. Division of Environmental Science and Engineering, Pohang University of Science and Technology, Pohang, S. Korea
2. Department of Atmospheric Sciences, Yonsei University, Seoul, S. Korea

*Corresponding author: Yign Noh (noh@yonsei.ac.kr)

Key Points:

- The spring phytoplankton bloom is realized by a newly developed Lagrangian plankton model coupled with large eddy simulation.
- A new criterion is suggested, which predicts the positive tendency of spring blooms in the high latitude ocean.
- Various statistics of Lagrangian particles, including the vertical migration of plankton, are investigated.

Abstract

A Lagrangian plankton model (LPM) is developed, in which the motion of a large number of Lagrangian particles, representing a plankton community, is calculated under the turbulence field simulated by large eddy simulation. A spring phytoplankton bloom is realized using the LPM, and the mechanism for its generation is investigated. Mixing by convective eddies during the night helps to maintain the uniform concentration of phytoplankton within the mixed layer, even if the daily mean surface heat flux is positive in spring. Accordingly, the spring bloom can be predicted by the critical depth hypothesis, if the mixing layer is used instead of the mixed layer. The shoaling of the mixing layer occurs immediately after the start of surface heating, but the shoaling of the mixed layer is delayed. A new criterion for the spring bloom is proposed, which predicts that spring blooms are more likely to occur at higher latitudes, even if the atmospheric forcing is the same. Furthermore, various statistics of Lagrangian particles, such as the vertical migration of plankton, the residence time of plankton within the euphotic zone, and the growth of plankton are investigated by taking advantage of the LPM.

Keyword: spring phytoplankton bloom, turbulence, large eddy simulation, Lagrangian plankton model, ocean mixed layer

Plain Language Summary

Phytoplankton concentrations increase rapidly in early spring in the high-latitude ocean. This is known as the spring bloom. This is because the surface mixed layer are shallower in spring at higher latitudes, and therefore phytoplankton spend more time under the sunlight, required for photosynthesis. A plankton model is developed, in which a large number of particles, representing a plankton community, move around in turbulent flows of the ocean. The spring bloom is simulated by the plankton model. The simulations show that the uniform concentration of phytoplankton is maintained near the sea surface, because of strong turbulent mixing generated during the night. Furthermore, results show that spring blooms are more likely to occur at higher latitudes, since the mixed layer depth tends to decrease with latitude in spring. A new criterion for the onset of the spring bloom is suggested. Furthermore, various statistics of plankton particles are investigated, such as the vertical migration of plankton, the residence time of plankton under sunlight, and the growth of plankton

1 Introduction

Spring phytoplankton blooms have long been of interest to oceanographers, not only from its importance in marine ecosystems and carbon cycling, but also as a fascinating example of the interaction between biological and physical processes in the upper ocean [e.g., Behrenfeld and Boss, 2014; Chiswell et al., 2015; Fischer et al., 2014]. It is usually observed in the high-latitude ocean, where the growth rate of phytoplankton concentration by photosynthesis is mainly controlled by the available light, and the seasonal variation of the mixed layer depth is large.

In order to explain the mechanism of its generation, Svedrup [1953] had earlier proposed the critical depth hypothesis (CDH) that the spring bloom occurs, if the mixed layer depth is shallower than the critical depth at which the vertically integrated phytoplankton growth and loss are balanced. For the evaluation of the critical depth, it is assumed that phytoplankton is well-mixed within the mixed layer and nutrients are abundant.

The CDH has since been widely used to predict spring phytoplankton blooms [e.g., Obata et al., 1996; Siegel et al., 2002]. Many observational evidences suggest, however, that the onset of spring blooms often precedes the shoaling of the mixed layer [Townsend et al. 1994; Dale et al., 1999; Eilertsen, 1993; Beherenfeld and Boss, 2014]. Such observations led Huisman et al. [1999] to propose the critical turbulence hypothesis (CTH) that, if vertical mixing is sufficiently weak, phytoplankton concentration is no longer uniform within the mixed layer, and near-surface blooms can take place, even if the mixed layer is still deep. This viewpoint has been taken in subsequent studies [Ebert et al., 2001; Chiswell 2011; Taylor and Ferrari, 2011; Brody and Lozier, 2014; Enriquez and Taylor, 2015; Kida and Ito, 2017].

There have been attempts to predict spring blooms in terms of the atmospheric condition such as the shutdown of surface cooling at the end of winter [Taylor and Ferrari, 2011; Ferrari et al., 2015] or the reduction of wind stress in spring [Chiswell et al., 2013]. Although the vertical mixing of phytoplankton is generally believed to be a key factor to generate spring blooms, there are also theories that consider other processes; for example, the decreasing grazing rate by zooplankton in the deep mixed layer during winter as a result of the diluted phytoplankton concentration [Behrenfeld 2010], or the conversion of lateral density gradients to stratification by sub-mesoscale eddies [Mahadevan et al. 2012]. These debates illustrate that further works are necessary to clarify the mechanism for the onset of spring blooms.

The temporal change of the horizontal mean phytoplankton concentration P can be described as

$$\frac{\partial P}{\partial t} = (\mu e^{-\lambda z} - m)P + \frac{\partial}{\partial z}\left(K \frac{\partial P}{\partial z} \right) \quad , \qquad (1)$$

where $\mu e^{-\lambda z}$ is the growth rate by photosynthesis, m is the loss rate by death, grazing and other processes, λ is the light attenuation coefficient, and K is an eddy diffusivity. Here we can define the spring bloom as a rise of P at the sea surface P_0 (= $P(z=0)$), i.e. $\partial P_0 / \partial t > 0$, following the onset of surface heating.

In the absence of vertical mixing (K = 0), the local balance $\mu e^{-\lambda z} = m$ is reached at $z = z_p$, which is called the compensation layer. The increase of P is possible below z_p,

however, in the presence of vertical mixing. If phytoplankton are well-mixed vertically ($\partial P/\partial z = 0$), the integration of $\partial P/\partial t$ up to the depth $z = z_c$ becomes zero, if

$$\frac{z_c}{1-e^{-\lambda z_c}} = \frac{\mu}{\lambda m} \quad . \tag{2}$$

(2) can be approximated as $z_c = \mu/\lambda m$, if $\lambda z_c >> 1$. Svedrup [1953] proposed that the spring bloom occurs, if the mixed layer depth becomes shallower than z_c, which is called the critical depth.

On the other hand, if turbulence is weak, the vertically uniform distribution of *P* cannot be maintained any more in the mixed layer. In this case a spring bloom can occur, if turbulent mixing is not strong enough to transport down the local phytoplankton accumulation near the sea surface, i.e., when

$$(\mu e^{-\lambda z} - m)P + \frac{\partial}{\partial z}\left(K\frac{\partial P}{\partial z}\right) > 0 \tag{3}$$

near the sea surface. They suggest that the CTH is applied when the mixed layer is deep and turbulence is weak, whereas the CDH is applied when the mixed layer is shallow and turbulence is strong [Huisman et al., 1999; Taylor and Ferrari, 2011; Enriquez and Taylor, 2015; Kida and Ito, 2017].

Both hypotheses usually presume that the mixing layer, where vertical mixing actually occurs, is the same as the mixed layer, where the uniform density is maintained. The mixed layer depth h_d is usually determined by the density difference from the sea surface, and the mixing layer depth h_m is usually determined by the decrease of *K* or the dissipation rate ε from the sea surface [e.g., Brainerd and Gregg, 1995; Noh and Lee, 2008; Sutherland et al., 2014]. They are not necessarily the same, however. For example, h_m can be much shallower than h_d in early spring, although they become equivalent ultimately with time, because the buildup of a sufficient density difference from the sea surface temperature at a certain depth takes time after the start of surface heating, whereas turbulence is weakened almost immediately [Brainerd and Gregg, 1993; Noh and Lee, 2008; Goh and Noh, 2013]. One can expect that the vertical migration of plankton is determined by the mixing layer, rather than the mixed layer. It has thus been pointed out that what triggers the spring bloom is the shoaling of the mixing layer, rather than the shoaling of the mixed layer, with respect to the CDH [Brody and Lozier, 2014; Franks, 2014; Enriquez and Taylor, 2015].

Both hypotheses illustrate that the most important factor to determine the onset of spring blooms is how effectively plankton migrate vertically, and therefore how much time they spend in the euphotic zone. The ideal approach for this is to track the motion of individual plankton as Lagrangian particles. It led several scientists to take the Lagrangian approach for the study of spring blooms [Woods and Onken, 1982; Kamykowski et al., 1994; Kida and Ito, 2017]. To our knowledge, all previous models calculate the vertical motion of Lagrangian planktons by random walks, however, instead of using the realistic turbulence field in the upper ocean.

Meanwhile, the progress in large eddy simulation (LES) now makes it possible to reproduce the realistic three-dimensional turbulent flow field of the ocean mixed layer [e.g., Noh et al., 2004; Sullivan and McWilliams, 2010]. LES has been extensively used to investigate the dynamical process of the ocean mixed layer. Recently, LES has been applied to study plankton dynamics by coupling to the biological process [Lewis, 2005; Taylor and

Ferrari, 2011; Enriquez and Taylor, 2015; Taylor, 2016; Brereton et al., 2018; Whitt et al., 2019]. In these LES models, however, the Eulerian approach is taken, in which the plankton concentration at a grid point is calculated. The motion of Lagrangian particles in the ocean mixed layer has been simulated by LES in order to understand the dispersion or settling of suspended particles, but the biological process has not been included so far [Noh et al., 2006, Noh and Nakada, 2010; Kukulka and Brunner, 2015].

The factors that are usually ignored in explaining the spring bloom are the diurnal variation and the latitudinal dependence of the mixed layer. Simulations are usually carried out without the diurnal cycle and at the fixed latitude. The mixed layer exhibits strong diurnal variation in terms of solar radiation and turbulent mixing, however. Solar radiation that allows the growth of phytoplankton is present only during the day, in which stratification, or a diurnal thermocline, suppresses the vertical motion of plankton. On the other hand, surface cooling during the night triggers convection that mixes phytoplankton over the whole mixed layer. Although there have been a few previous attempts [Wood and Onken, 1982; Taylor and Stephens 1993], the role of the diurnal variation of the mixed layer in the spring bloom is not yet clearly understood.

Recently, Goh and Noh [2013] showed using LES that a seasonal thermocline is formed at a certain depth in the extratropical ocean, across which the downward transports of heat and momentum are prohibited, but heat and momentum continue to propagate downward to the deeper ocean without forming a well-defined thermocline in the equatorial ocean. The Coriolis force limits the downward transport of momentum to the Ekman length scale. As a result, in the absence of velocity shear below the Ekman length scale, the positive feedback between turbulence and stratification leads to the formation of a seasonal thermocline at a certain depth. In the absence of the Coriolis force, however, turbulent kinetic energy is maintained at a certain level at every depth, because the buoyancy decay is balanced by the enhanced shear production. The depth of a seasonal thermocline h_s is then predicted by [Goh and Noh, 2013]

$$h_s = Cu_*^2 / (fQ_0)^{1/2} \quad , \tag{4}$$

where h_s is calculated by the maximum density gradient, u_* is the frictional velocity, Q_0 is the surface buoyancy flux, f is the Coriolis parameter, and C = 0.5. The scaling (4) is in contrast to the traditional Monin-Obukhov scaling as $h_s \sim u_*^3 / Q_0$, suggested by Kraus and Turner [1967] for the depth of a seasonal thermocline, but it is confirmed from the recent analysis of climatological data [Yoshikawa, 2015; Lee et al. 2015]. The scaling (4) implies that the onset of spring blooms may appear differently at different latitudes, even if all other conditions are the same.

In the present work we apply a newly developed Lagrangian plankton model (LPM), in which Lagrangian plankton particles move in the realistic turbulence field of the ocean mixed layer, simulated by LES, while undergoing the biological process. The simulation concerns the condition in which a seasonal thermocline is formed, similar to Goh and Noh [2013], and includes the diurnal variation. Results are analyzed to examine existing theories, such as CDH and CTH, and to investigate the effect of the latitudinal dependence. A new criterion is proposed for the onset of spring blooms based on it. Furthermore, various statistics of Lagrangian particles, such as the vertical migration of plankton, the residence time of plankton within the euphotic zone, and the growth of plankton are also investigated.

2. Model and Simulation

2.1 Model

The LES model used in the present simulation is similar to those used in Noh et al. [2004, 2006, 2011], which has been developed based on PALM (PArallelized LES Model) [Maronga et al, 2015]. Langmuir circulations are realized by the Craik-Leibovich vortex force [Craik and Leibovich, 1976], and wave breaking is represented by stochastic forcing. The wave length and height used for the Stokes velocity in the vortex force are fixed as 40 m and 0.5 m, respectively, as in previous works.

Each Lagrangian particle represents a large number of plankton that follow the same trajectory, which is called a plankter for convenience in the present paper. The velocity of a plankter is determined by the interpolation of the fluid velocity at the neighboring grid points [Noh et al., 2006; Noh and Nakada, 2010]. The interpolation scheme for particle velocity is devised to ensure that particles follow the incompressibility condition of the flow [Grabowski et al., 2018]. Sinking of a plankter is not considered in the present work.

Each Lagrangian particle experiences the biological process of phytoplankton as

$$\frac{dp_i}{dt} = (\mu e^{-\lambda z} - m)\, p_i \quad , \tag{5}$$

where p_i is the biomass of a plankter. The summation of all p_i within a grid divided by the grid volume provides the phytoplankton concentration. The equation for P can then be expressed as

$$\frac{\partial P}{\partial t} = -\frac{\partial}{\partial z}\overline{P'w'} + \left(\mu e^{-\lambda z} - m\right) P \, , \tag{6}$$

under the condition of horizontal homogeneity, if the number of particles per grid becomes sufficiently large. Here $\overline{P'w'}$ is the vertical flux of phytoplankton concentration induced by the vertical fluctuation of Lagrangian particles. If $-\overline{P'w'} = K\partial P / \partial z$ is assumed, (6) becomes equivalent to (1).

The Lagrangian plankton model can realize more naturally plankton dynamics, as each plankter experience the biological process responding to the background condition, while following the fluid motion. Turbulent diffusion of plankters can be realized by the motion of particles without introducing the mixing coefficient. It can also be naturally extended to include the processes such as sinking, swimming, and aggregation [e.g., Jokulsdottir and Archer, 2016]. The Lagrangian plankton model allows us to trace the location and growth of plankters, thus giving us critical information for the spring bloom, in particular.

2.2 Simulation

Simulation of the mixed layer is carried out to reproduce the formation of a seasonal thermocline under surface heating in spring from the deep mixed layer produced under surface cooling in winter. The surface heat flux, including the diurnal variation, is given by $\tilde{H}_0 = A\sin(2\pi t/T)$, but by $\tilde{H}_0 = -B$, if $A\sin(2\pi t/T) < -B$, where T is 1 day (Figure 1). For the first two days, integration is carried out under the winter condition with the negative daily mean surface heat flux (H_0 < 0 Wm^{-2}), starting with the initial mixed layer depth 120 m and N^2 = 10^{-4} s^{-2} for stratification below. After two days, H_0 is switched to the spring condition with the positive daily mean heat flux (H_0 > 0 Wm^{-2}), and integration is carried out for another 10 days, which is expected to be sufficient to reproduce the essential dynamics of seasonal thermocline formation [Goh and Noh, 2013]. Under the spring condition, A and B are 400 and 100 Wm^{-2}, resulting in H_0 = 81.3 Wm^{-2}, corresponding to the surface buoyancy flux Q_0 = 4.97× 10^{-8} m^{2}s^{-3}. Under the winter condition, both values of A and B decrease by the same amount so as to produce H_0 = – 81.3 Wm^{-2}. The model domain is 300 m horizontally and 180 m vertically, and the grid size is 1 m in all directions.

The parameters used for the biological process (5) are given by m = 0.1 d^{-1}, and λ = 10^{-1} m^{-1}. For the calculation of photosynthesis we take into account the diurnal variation, so μ = 2 d^{-1} during the day ($\sin(2\pi t/T) > 0$) and μ = 0 d^{-1} during the night ($\sin(2\pi t/T) < 0$). It results in the critical depth z_c = 50 m. Parameter values of m, λ, and z_c are the same as in Taylor and Ferrari [2011]. Since we focus on the short period at the onset of a spring bloom, we assume that nutrients are abundant and invariant in time, and neglect the interactions between phytoplankton, zooplankton, and nutrients. Therefore, μ and m are constant, as in previous simulations [Wood and Onken, 1982; Taylor and Ferrari, 2011; Enriquez and Taylor, 2015]. 10^5 particles are released initially at z = 5 m at the start of simulation (t = – 2 day). Convective mixing during the night of the first day mixes particles uniformly within the mixed layer. p_i and P represent the normalized value with respect to the initial values, i.e. $p_i = P = 1$ at t = – 2 day. Simulations are carried out with different wind stress (u_* = 0.007, 0.01, 0.015, 0.02 ms^{-1}) and latitudes (ϕ = 0, 20, 40 °N).

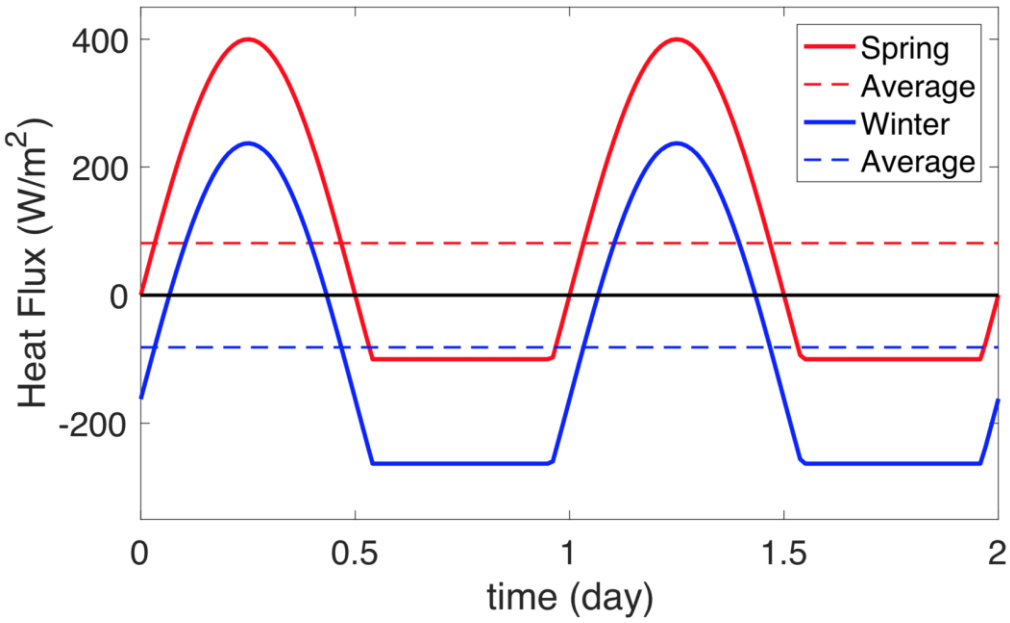

Figure 1 Diurnal variation of surface heat flux (red: spring, blue: winter)

3. Results

3.1 Evolutions of Buoyancy, Dissipation Rate, and Phytoplankton Concentration.

Figure 2 compares the evolutions of buoyancy *B*, the dissipation rate ε, and *P* for three different cases; the control simulation (CON: ϕ = 40°N, u_* = 0.01 ms^{-1}), the strong wind case (SW: ϕ = 40°N, u_* = 0.02 ms^{-1}), and the equatorial case (EQ: ϕ = 0°, u_* = 0.01 ms^{-1}). The corresponding times series of h_m, h_d, and P_0 are shown in Figure 3. Here h_d is determined by the difference of density from the surface $\Delta\rho$ = 0.1 kgm^{-3}, corresponding to ΔB = 9.8 × 10^{-4} ms^{-2}, and h_m is determined by the depth at which ε < 10^{-8} m^{2}s^{-3}, based on the typical values used in the analysis [Noh and Lee, 2008; Sutherland et al., 2014]. Also included are h_s and z_c for reference. Here h_s is calculated by the maximum N^2 at the last night (*t* = 9.75 day), as in Goh and Noh [2013].

At CON, a seasonal thermocline is formed, across which the downward transports of heat and momentum are prohibited, as shown in Goh and Noh [2013], after the start of the spring condition (H_0 > 0 Wm^{-2}). The evolutions of *B* and ε reveal two important features. First, the suppression of turbulence, or the decrease of ε, occurs almost immediately after the start of surface heating, but the appearance of ΔB larger than the threshold value takes time. Therefore $h_m < h_d$ in the early stage of surface heating, while $h_m \sim h_d$ is approached ultimately with time (Figure 3). It is a robust feature regardless of the threshold values of ΔB and ε, although the period with $h_m < h_d$ may vary. Second, stratification appears within the mixed layer during the daytime, associated with the formation of a diurnal thermocline [Noh et al., 2009; Brainerd and Gregg, 1993]. It causes the diurnal cycle of h_m, and h_m becomes equivalent to h_s, or h_d, only during the night. In the present paper we use the term the mixed layer, once $h_m \sim h_d$ is reached. Note that h_d has no diurnal variation.

h_m is much deeper at SW, as expected from (4), and it takes much longer to make ΔB large enough to produce h_d. On the other hand, at EQ, *B* continues to propagate downward to the deeper ocean without forming a well-defined thermocline, as shown in Goh and Noh [2013]. Therefore, h_m continues to increase with time indefinitely, and h_d is not produced for 10 days (Figure 3).

At CON and SW, the vertical gradient of *P* appears within the mixed layer during the daytime, when $h_m \sim h_d$, since vertical mixing of plankton is suppressed by stratification. On the other hand, *P* becomes uniform within the mixed layer during the night. It implies that plankters are mixed completely over the whole mixed layer depth by convective eddies during the night when there is no photosynthesis. It provides the condition, in which the CDH can be applied. Meanwhile, Figure 3 shows that the increase of P_0 responds to the decrease of h_m, rather than h_d. At CON, P_0 starts to increase as soon as h_m decreases, while h_d still remains large. It explains many observations that the onset of the spring bloom precedes the shoaling of the mixed layer [Townsend et al. 1994; Dale et al., 1999; Eilertsen, 1993]. It also confirms the argument that the onset of the spring bloom is due to the decrease of h_m, rather than the decrease of h_d [Brody and Lozier, 2014; Franks, 2014; Enriquez and Taylor,

2015]. h_m is smaller/larger than z_c (= 50 m) at CON/SW, respectively. Accordingly, P_0 increases with time at CON, thus generating a spring bloom, while P_0 decreases with time at SW. On the other hand, there appears a significant vertical gradient of *P* over the whole depth at EQ, contrary to the cases at ϕ = 40°N (CON, SW). It implies that the CDH cannot be applied in this case. The cases SW and EQ show clearly that the shutdown of convection under the surface heating does not always induce a spring bloom, contrary to Taylor and Ferrari [2011].

Figure 4 shows the distribution of plankters together with vertical velocity at the vertical cross-section for three cases at the night of a winter day (t = – 0.25 day) and a spring day (t = 9.75 day). The patterns on a winter day are similar in all three cases, although the intensity of vertical mixing is different, so only the case of CON is shown from now on. On a winter day, p_i of each plankter is rather uniform, because of the short period of change from the initial value. On a spring day of CON and SW, plankters are divided to two groups; large p_i within the mixed layer and very small p_i below the mixed layer. It also shows that two groups are not mixed to each other. On the other hand, at EQ, p_i tends to decrease slowly with depth, and shows a large variance. It suggests that each plankter experiences a different time history of growth during the daytime, while they are mixed together during the night. Figure 3 also shows that p_i does not show any correlation with the velocity field, because the time scale of plankton growth is much longer than the mixing time scale.

The tracks following the depth of a plankter z_i illustrate the vertical migration of sampled plankters during one day (Figure 5). Here the color of tracks represents the depth of a plankter at the start of the day. On a winter day (t = − 1 day), it shows clearly that plankters are separated by the diurnal thermocline (*z* ~ 20 m) with the weak vertical velocity during the daytime, they are mixed completely by strong vertical velocity during the night (Figure 5a). On a spring day (t = 10 day) of CON, plankters in the mixed layer above the seasonal thermocline and below it are clearly decoupled. Plankters show almost no vertical motion below the mixed layer, reflecting very weak turbulence there. Even within the mixed layer, plankters are separated to above and below the diurnal thermocline during the daytime, before mixing together over the whole mixed layer during the night. It confirms that each plankters experiences a different growth rate during the daytime, but they are mixed together during the night, as shown in Figure 3. The similar pattern is found at SW, although the vertical motion is stronger, and the depth of a diurnal thermocline is deeper. Furthermore, in this case a small fluctuation exists below the mixed layer associated with internal waves generated by strong turbulence impinging on the mixed layer [Polton et al., 2008; Czeschel and Eden, 2019]. Its existence can also be confirmed from the distribution of ε below the mixed layer (Figure 2b). On the contrary, on a spring day of EQ, no decoupling across the seasonal thermocline occurs, and vertical mixing occurs over the whole depth. The magnitude of vertical fluctuation is smaller than on a winter day, however.

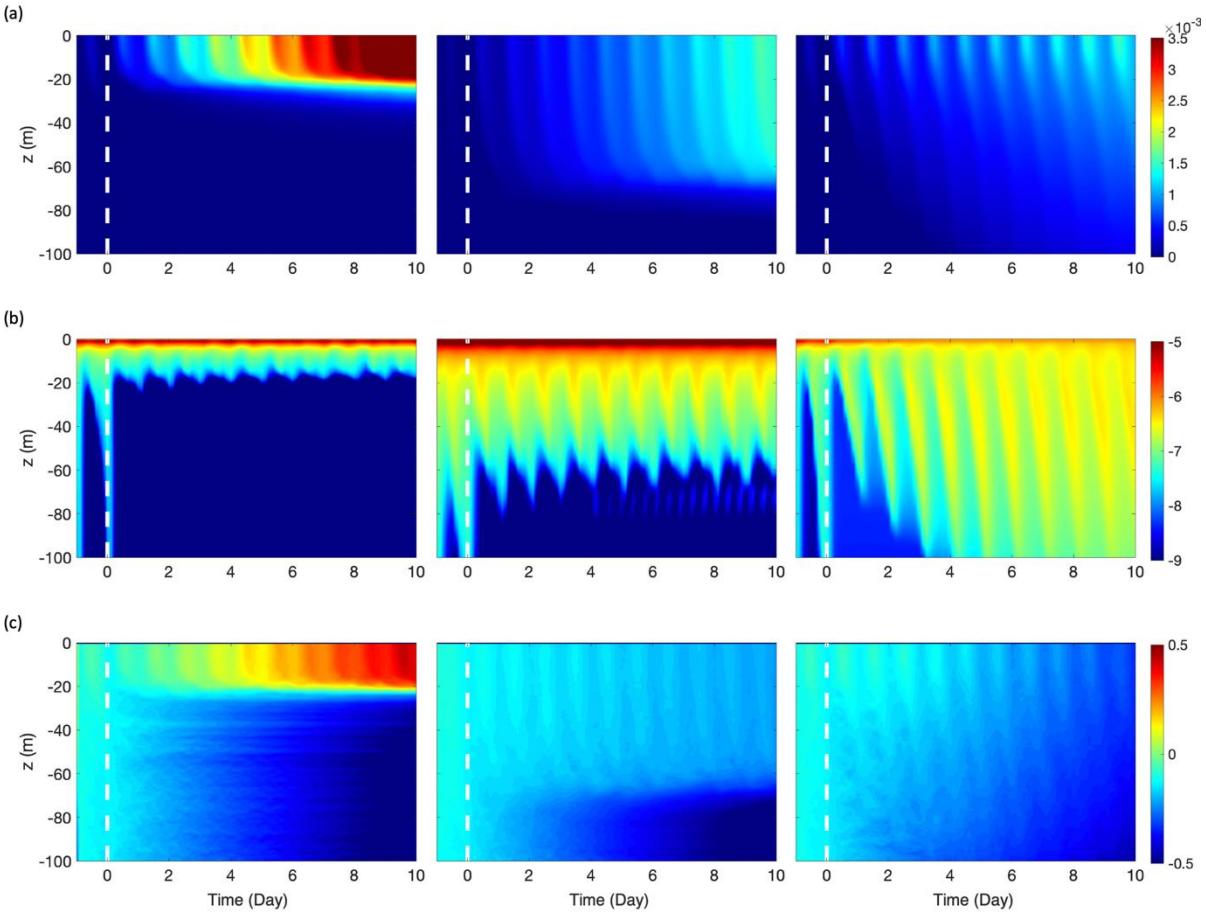

Figure 2 Time series of profiles (CON: left, SW: middle, EQ: right). Q_0 changes from negative to positive at t = 0 day (dashed line) : (a) B, (b) ε, (c) log(P).

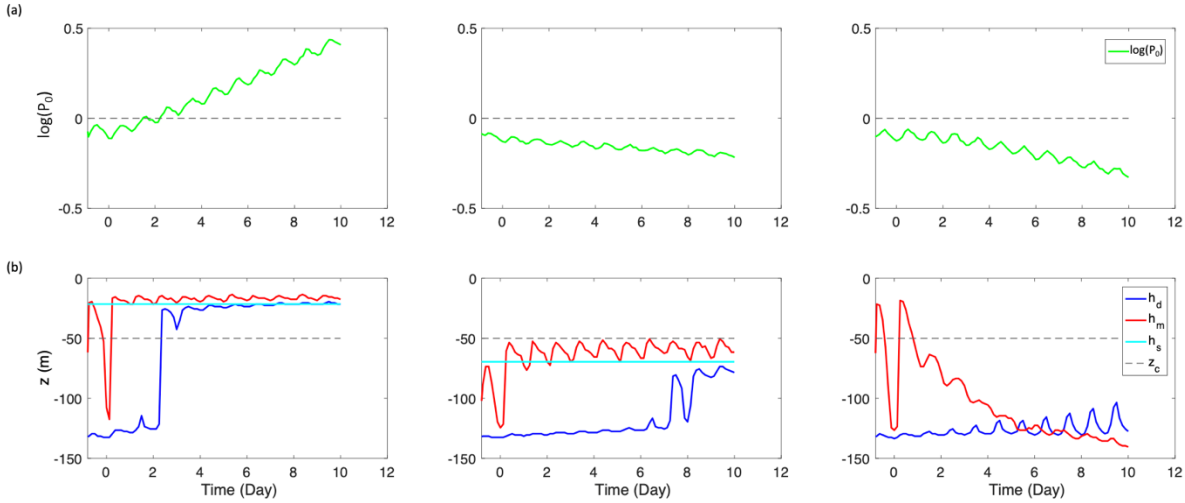

Figure 3 Time series (CON: left, SW: middle, EQ: right): (a) $\log(P_0)$, (b) the mixing layer depth h_m (red), the mixed layer depth h_d (blue), the depth of a seasonal thermocline h_s (sky blue horizontal line), and the critical depth z_c (horizontal dashed line) (h_s is calculated at t = 9.75 day by the maximum N^2).

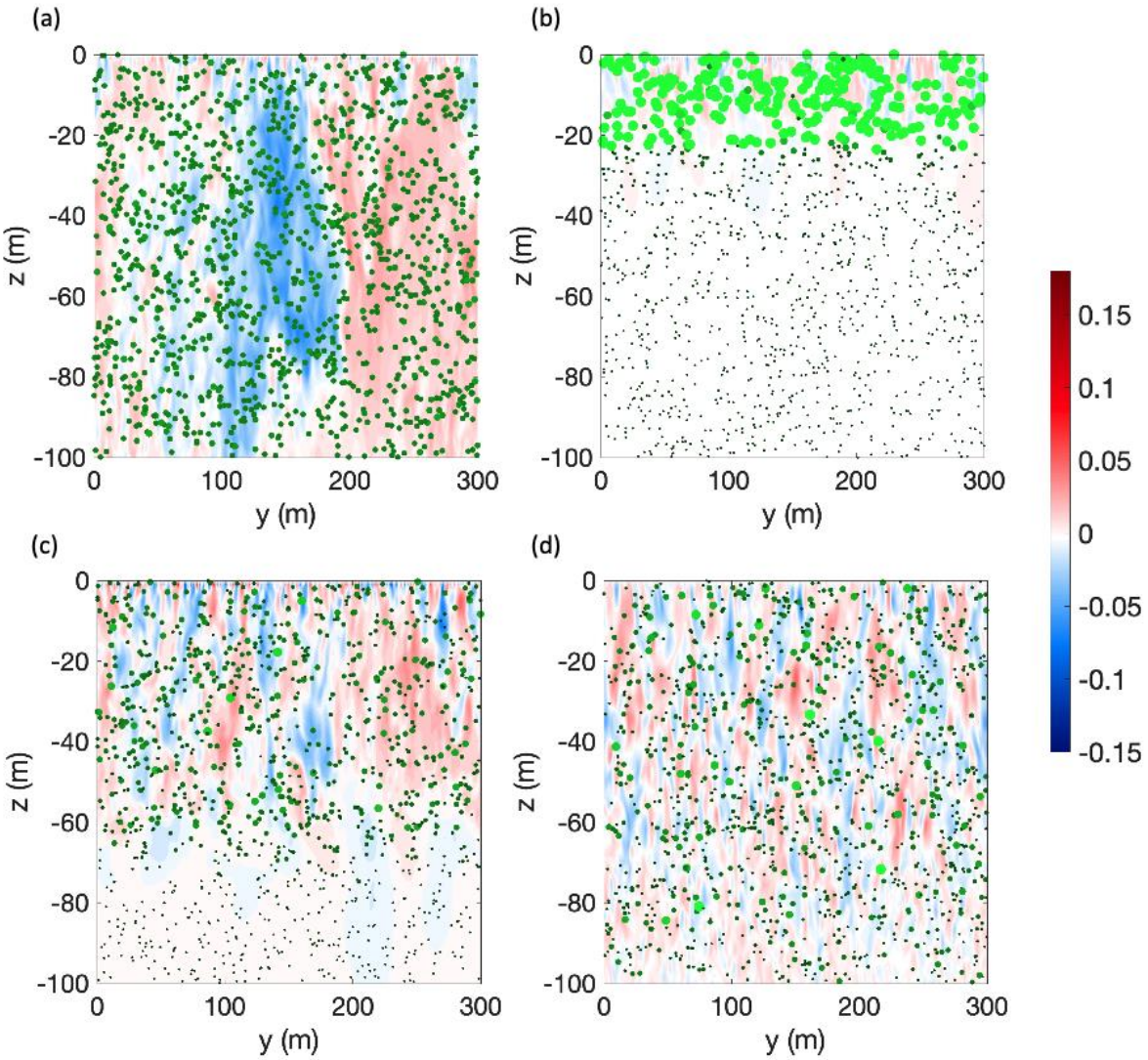

Figure 4 Distributions of instantaneous vertical velocity and plankters. The size of a plankter represents p_i: (a) CON (t = – 0.25 day), (b) CON (t = 9.75 day), (c) SW (t = 9.75 day), (d) EQ (t = 9.75 day).

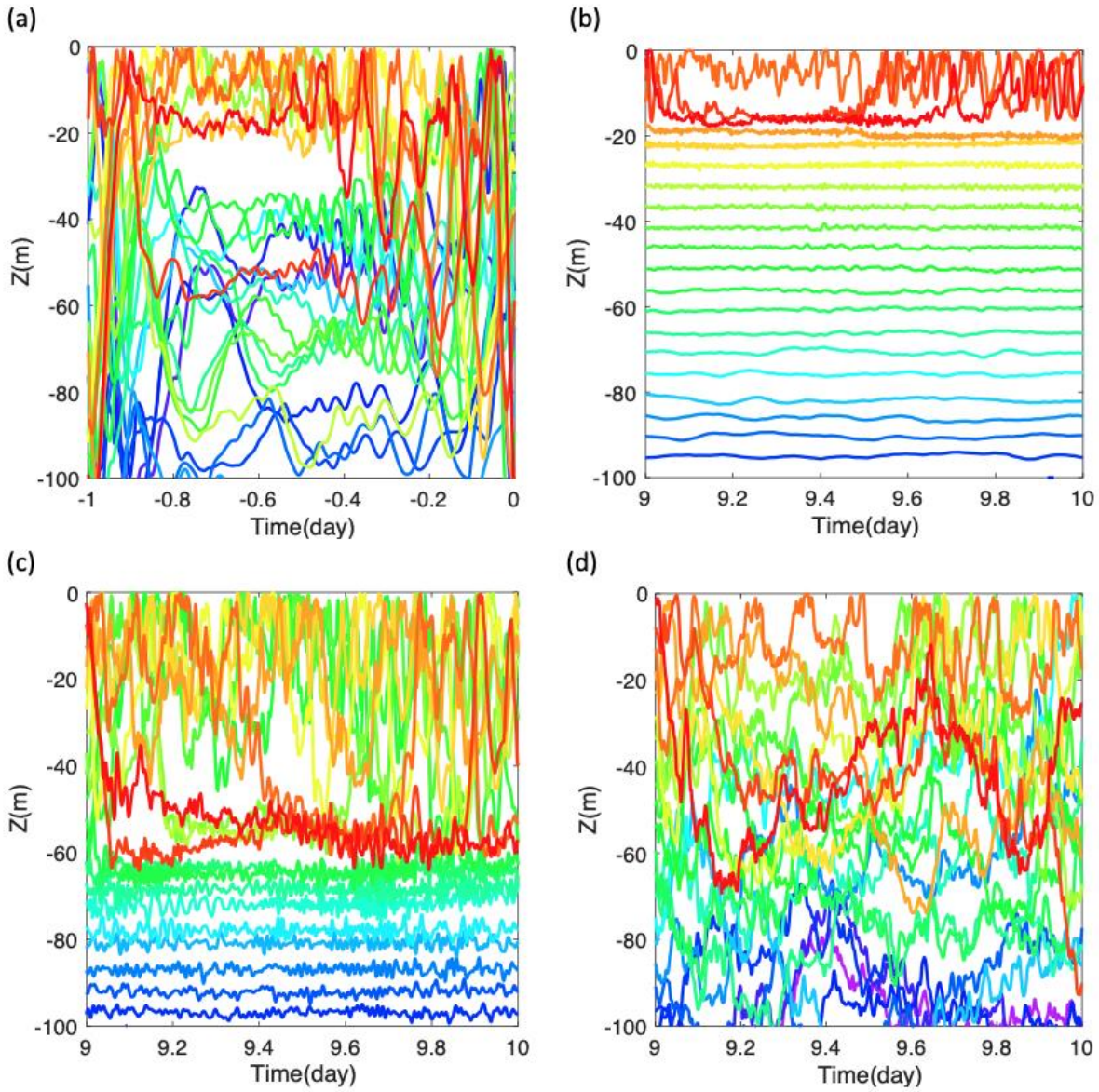

Figure 5 Tracks of vertical position (z_i) of sampled plankters during one day (The color of a track represents the initial depth of a plankter at the start of the day.): (a) CON (t = – 1 day), (b) CON (t = 10 day), (c) SW (t = 10 day), (d) EQ (t = 10 day).

3.2 Lagrangian Statistics of Plankters

The Lagrangian plankton model allows us to analyze the motion and growth of individual plankters directly. We obtain the probability distribution function (PDF) of the range of vertical migration during one day $n_z\Delta z$, the residence time of a plankter within the euphotic zone during one day τ_r, and the daily mean p_i of the last day (t = 10 day) (Figures 6, 7, and 8) for the corresponding cases shown in Figure 4 and 5. Here n_z is the number of grids covered by the vertical migration of plankters during one day and Δz = 1 m. Color assigned to each value of $n_z\Delta z$, τ_r, and p_i represents the average depth of plankters belonging to that value.

On a winter day, the maximum frequency of $n_z\Delta z$ occurs near $n_z\Delta z \sim h_d$ (h_d □ 130 m), albeit slightly smaller (Figure 2), as expected from the fact that the mixing length l_m of convective eddies is comparable to h_d (Figure 6). It is consistent with the relation $l_m \sim h_d$ obtained from the analysis of Lagrangian float data under the daily mean surface cooling in the real ocean [Brody and Lozier, 2015]. Figure 1a also reveals, however, that $n_z\Delta z$ is smaller than h_d for a large number of plankters, which possibly raises questions about the applicability of the CDH. On a spring day of CON and SW, plankters are divided into two groups, $n_z\Delta z \sim h_d$ and $n_z\Delta z \sim 0$ m. It means that plankters within the mixed layer migrates over the whole mixed layer depth during the night, while plankters below the mixed layer remains almost motionless. It is also important to note that $n_z\Delta z$ is somewhat smaller than h_s or h_d. The vertical motion is suppressed both near the sea surface and near the bottom of the mixed layer, thus making $n_z\Delta z < h_s$. At SW, $n_z\Delta z$ below the mixed layer shows values larger than zero, reflecting the effect of internal waves. Brody and Lozier [2015] suggested that the mixing length is proportional to the Ozmidov length scale ($l_m \sim \varepsilon^{1/2}N^{-3/2}$) under the daily mean surface heating, but the present result suggests that the mixing length relevant to the vertical migration of phytoplankton during one day is that of convective eddies during the night even under the daily mean surface heating; i.e., $l_m \sim h_d$. On the other hand, at EQ, much wider variance of $n_z\Delta z$ is observed, while the mean value is much smaller than h_m (~ 140 m). The relation $l_m << h_m$ leads to the appearance of the vertical gradient of P, as shown in Figure 2c. It is also found that $n_z\Delta z$ decreases with depth at z > 50 m, indicating the weakening turbulence with depth.

Figure 6 shows the PDF of τ_r. Here τ_r is calculated only during the daytime when μ = 2, and the euphotic zone is defined by the compensation depth (z_p = 23 m), as in Kida and Ito [2017]. On a spring day of CON, τ_r is divided into two groups of plankters; τ_r = 0 hr and τ_r = 12 hr. It is due to the fact that z_p happens to be very close to h_d in this case. As a result, plankters in the mixed layer always reside in the euphotic zone, and those below the mixed layer always reside below the euphotic zone. In other cases (Figure 7a, c, and d), $h_d > z_p$, and it results in the broader distribution of τ_r. Plankters in the mixed layer migrates vertically, above and below z_p, although the vertical motion is rather

suppressed by stratification during the daytime. Sometimes they make multiple entry to the euphotic zone, as suggested by Kida and Ito [2017].

Finally, the PDF of p_i is directly related to the onset of spring blooms. Unlike $n_z \Delta z$ and τ_r, it represents the integrated property over 12 days, starting with p_i = 1. Therefore, on a winter day, the variance of p_i is small, and its mean value is close to the initial value. On a spring day at CON, p_i is larger than one for plankters in the mixed layer, and it is smaller than one below the mixed layer, as shown in Figure 4. The variance of p_i is large for the former, indicating the different history of growth for each plankter during the daytime at each day. A plankter can reside randomly either above or below the diurnal thermocline at each day, while it is mixed over the whole mixed layer during the night. The distribution of p_i is divided into two groups at SW too, but the values of p_i are smaller than one for plankters, including the one in the mixed layer, as expected from Figure 2. The distribution of p_i at EQ also shows that p_i is smaller than one for most plankters, and p_i tends to decrease with depth.

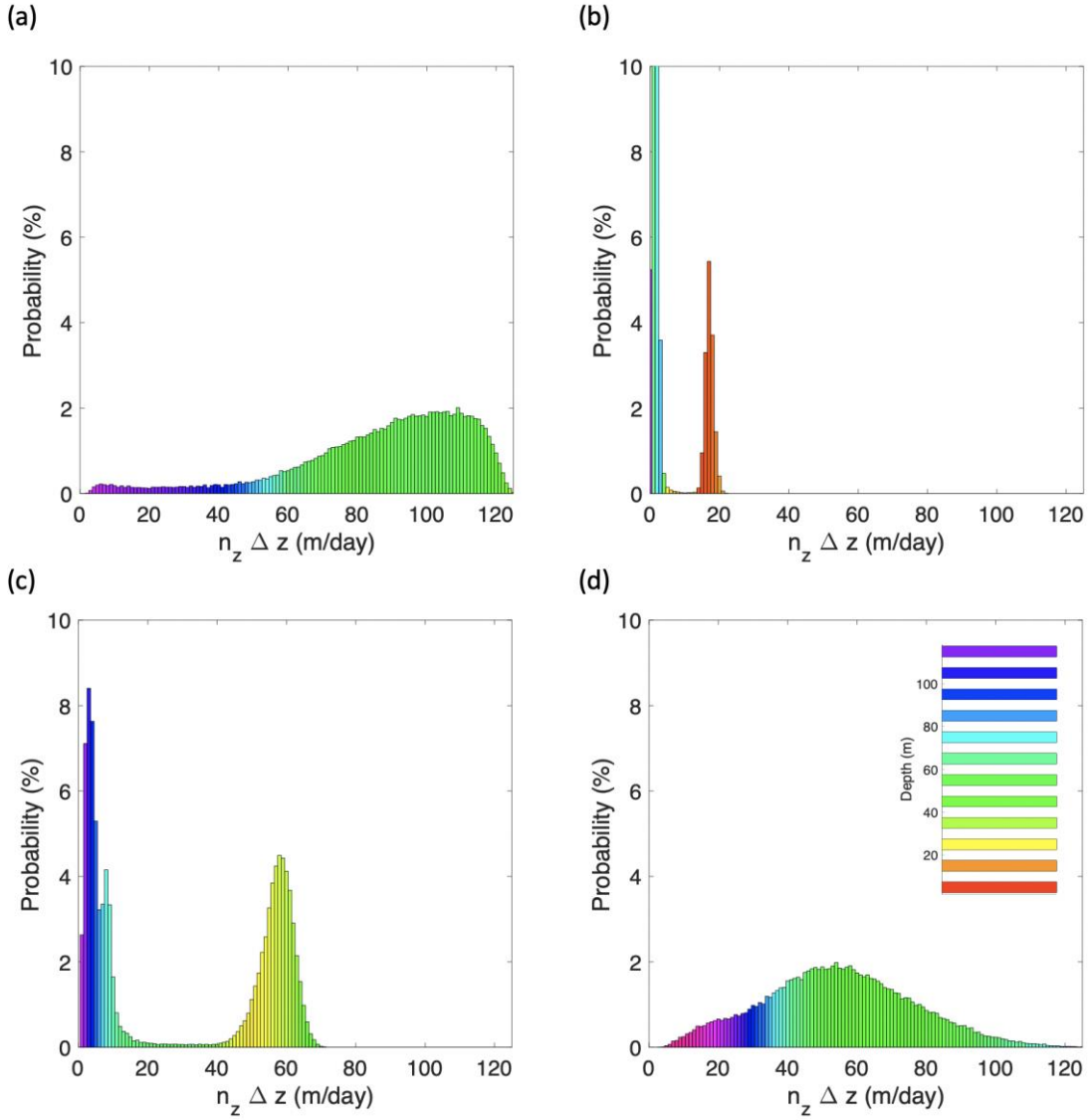

Figure 6 Probability distribution function of the number of grids $n_z\Delta z$ visited by a plankter during one day (The average depth of particles belonging to each $n_z\Delta z$ is represented by color): (a) CON (t = – 1 day), (b) CON (t = 10 day), (c) SW ((t = 10 day), (d) EQ (t = 10 day).

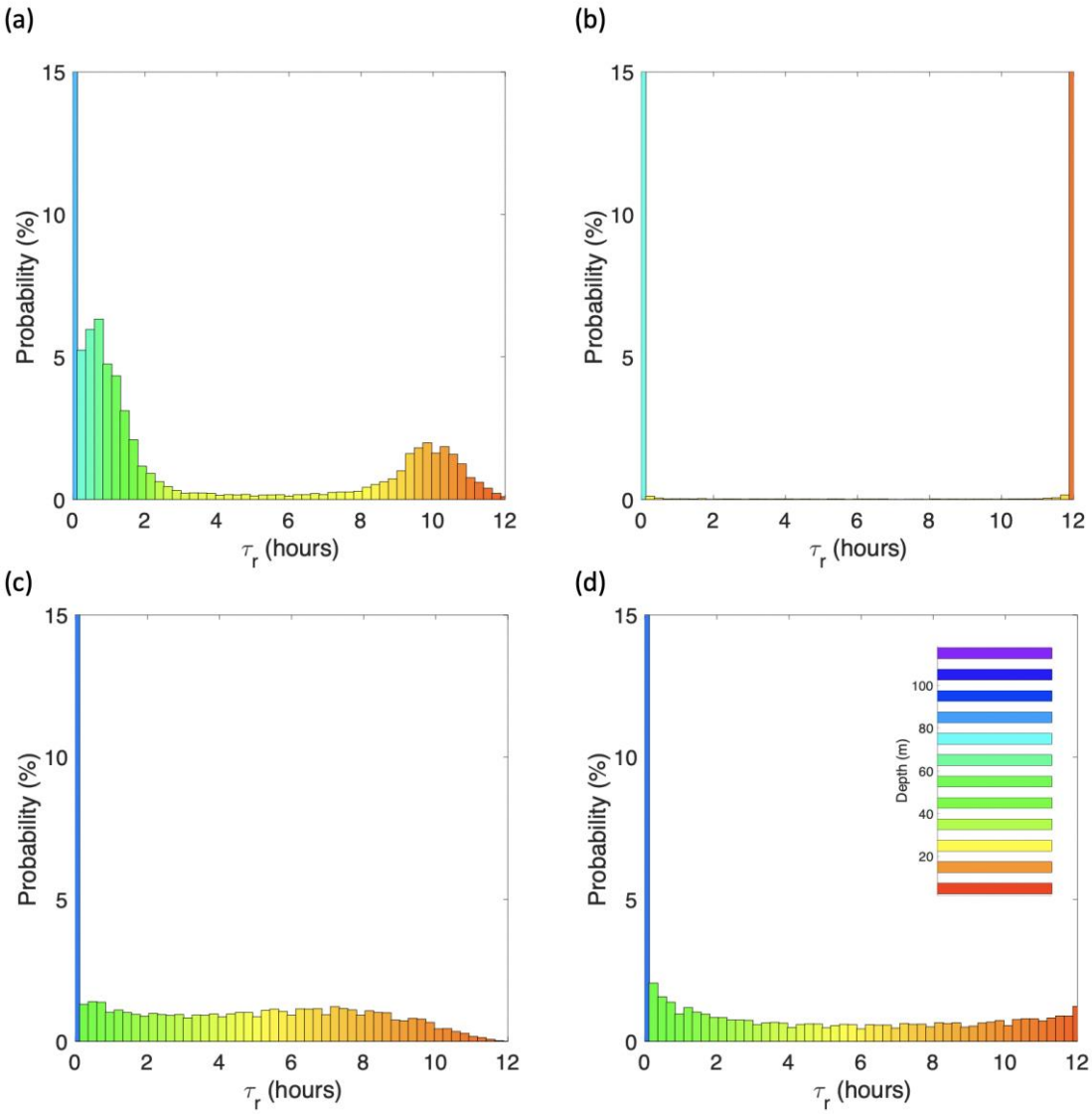

Figure 7 Probability distribution functions of the residence time (τ_r) of a plankter within the euphotic zone during one day (The average depth of particles belonging to each τ_r is represented by color): (a) CON (t = – 1 day), (b) CON (t = 10 day), (c) SW ((t = 10 day), (d) EQ (t = 10 day).

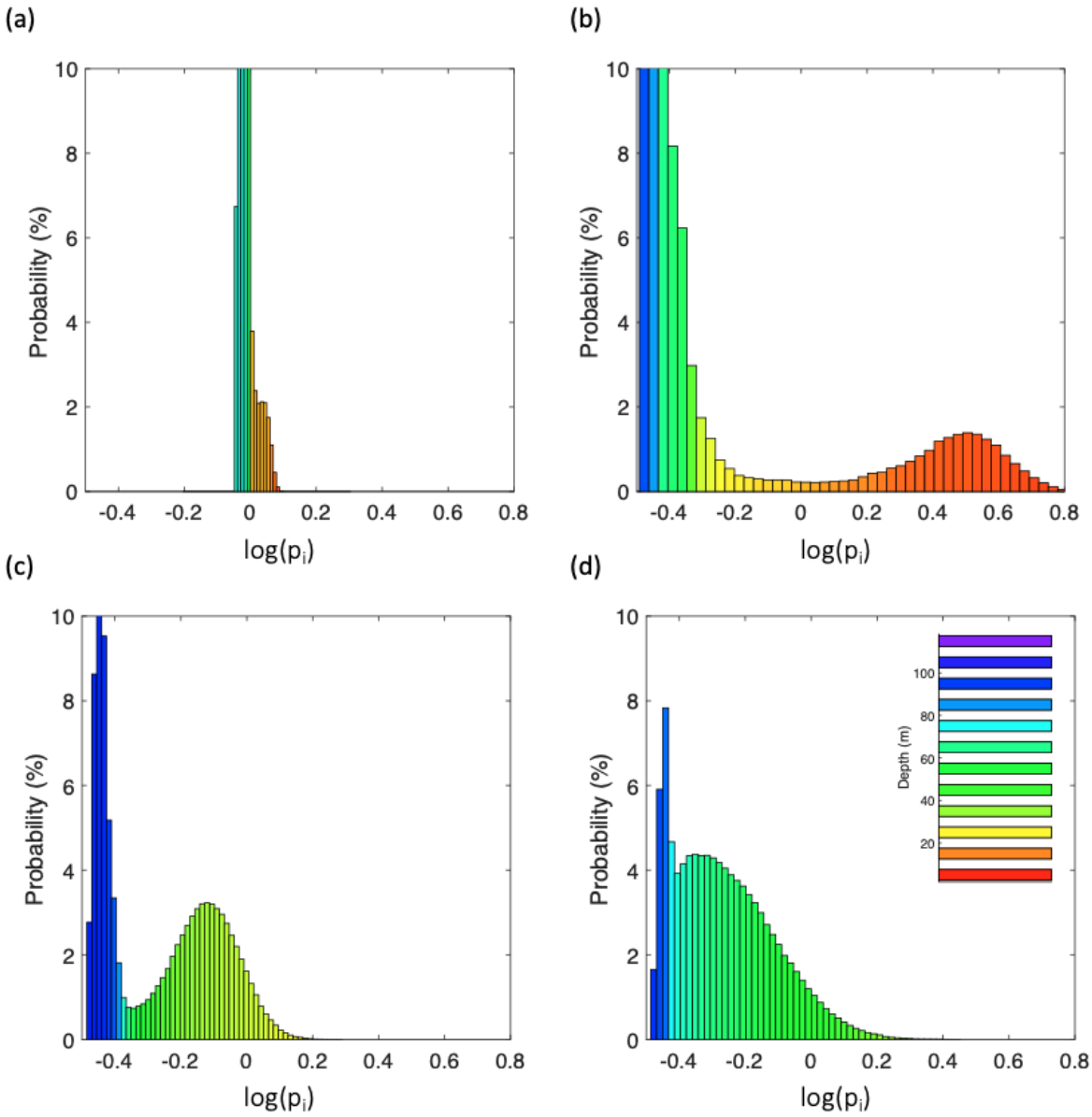

Figure 8 Probability distribution function of $\log(p_i)$ averaged over a day (The average depth of particles belonging to each $\log(p_i)$ is represented by color): (a) CON (t = – 1 day), (b) CON (t = 10 day), (c) SW (t = 10 day), (d) EQ (t = 10 day).

3.3 Criterion for the Onset of a Spring Bloom

The analysis in the previous section reveals several important features of the spring bloom. First, the decrease of h_m appears as soon as the surface heating starts, while the decrease of h_d appears after some time. The increase of P_0 starts simultaneously with the decrease of h_m if $h_m < z_c$ (CON). Second, convective eddies mix plankters over the whole mixed layer during the night, when there is no growth of phytoplankton. These features suggest that the CDH can be applied to predict a spring bloom, if the mixing layer is used instead of the mixed layer.

Furthermore, if h_s is used for h_m, the criterion for the onset of a spring bloom $h_m < z_c$ can be rewritten as

$$u_*^2 < (fQ_0)^{1/2} \lambda\mu / (Cm), \qquad (7)$$

using the relation (4). Figure 9 shows the difference of the daily mean $\log P_0$ between t = 1 and 10 day, $\Delta \log P_0$, from each simulation with different f and u_*, together with the dashed line representing the criterion (7). $\Delta \log P_0$ confirms the relation (7) with C = 0.3, which is somewhat smaller than that used for h_s (C = 0.5). It reflects the fact that $n_z \Delta z$ tends to be smaller than h_s (Figure 6), and that the vertical gradient of P appears within the mixed layer during the daytime, which makes the daily mean P_0 larger.

The criterion (7) indicates that the intensity of a spring bloom, represented by $\Delta \log P_0$, becomes larger at higher latitudes, even if all other conditions are the same. It is worthwhile to mention that Enriquez and Taylor [2015] also proposed the criterion in which the critical u_*^2 increases with f and Q_0, similar to (7). However, their criterion is based on the CTH, and they did not examine the latitudinal dependence and the effect of diurnal variation. It is also necessary to remind that, in the real ocean, limited nutrient supply and the weak seasonal variation of the mixed layer depth are more important reasons to prohibit the onset of spring blooms at low latitudes.

The CTH usually assumes that K and h_d are independent parameters. For example, it is suggested that the CTH is applied for small K and large h_d, and the CDH is applied for large K and smaller h_d [Huisman et al., 1999; Taylor and Ferrari, 2011; Enriquez and Taylor, 2015; Kida and Ito, 2017]. However, K and h_d are not independent parameters. Larger u_* makes K and h_d larger simultaneously during the formation of a seasonal thermocline. Moreover, the CTH does not take into account the diurnal variation of the mixed layer. Convective eddies mix plankters over the whole mixed layer during the night, when there is no growth of phytoplankton. It means that the mixing time scale is always much shorter than the growth time scale in this case, thus contradicting the basic assumption for the CTH.

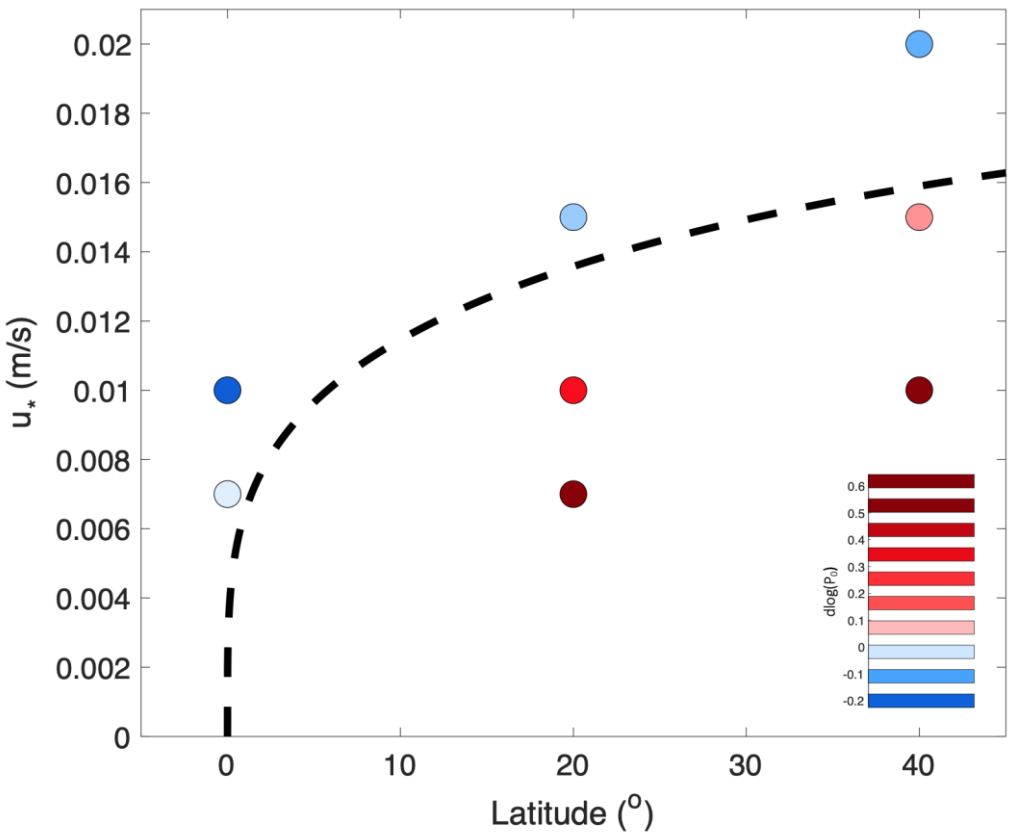

Figure 9 The difference of the daily mean $\log P_0$ between t = 1 and 10 day, $\Delta \log P_0$, from simulations with different u_* and f (A dashed line is the criterion (7) with C = 0.3)

4. Conclusion

In the present work, a Lagrangian plankton model is developed, in which the motion of a large number of Lagrangian particles, representing a plankton community, is calculated under the turbulence field of the ocean mixed layer simulated by LES. The Lagrangian plankton model is applied to reproduce a spring bloom following the onset of surface heating and the formation of a seasonal thermocline successfully. The mechanism for the spring bloom is clarified based on the analysis of model results, and a new criterion is proposed for the onset of a spring bloom. The main results are summarized as below.

First, the onset of spring blooms can be predicted by the critical depth hypothesis (CDH), if the mixing layer is used instead of the mixed layer. The shoaling of the mixing layer occurs immediately after the start of surface heating, but the shoaling of the mixed layer is delayed. It explains the observation of spring blooms preceding the shoaling of the mixed layer.

Second, convective eddies mix plankters over the whole mixed layer during the night. Accordingly, one can apply the CDH based on the uniform P within the mixed layer, even if the daily mean surface heat flux is positive.

Third, a new criterion for the onset of the spring bloom is proposed based on the CDH using the scaling for the depth of a seasonal thermocline, proposed by Goh and Noh [2013]. It suggests that spring blooms are more likely to occur at higher latitudes, even if the atmospheric forcing is the same. In the equatorial ocean, a seasonal thermocline is not formed, and therefore spring blooms cannot occur regardless of the atmospheric forcing.

Fourth, the range of vertical motion of plankters during one day in the mixed layer is comparable to h_d, albeit slightly smaller, both under the daily mean surface cooling and heating. In the equatorial ocean, however, it is much smaller than h_m.

Finally, a large variance of p_i appears in the mixed layer, since each plankter experiences a different time history of growth during the daytime, while they are mixed together during the night.

The present work shows that the Lagrangian plankton model is a powerful tool to study plankton dynamics. The model is naturally capable of extending further to include interactions between phytoplankton, zooplankton, and nutrients. Furthermore, the model provides a natural basis to explore processes such as sedimentation and aggregation.

Acknowledgments

This work was supported by the Korea Meteorological Administration Research and Development Program under Grant KMI2018-07210. Most of the simulations have been carried out on the supercomputer system supported by the National Center for Meteorological Supercomputer of Korea Meteorological Administration (KMA). We also appreciate the support of Prof. Naoki Hirose, RIAM, Kyushu University, Japan, in setting up the condition to start this research. The PALM code is available on the link https://palm.muk.uni-hannover.de/trac), and all the data used in this study are available on the link (https://figshare.com/articles/Lagrangian_Plankton_Model/11924142).

References

Behrenfeld, M. J. (2010). Abandoning Sverdrup's Critical Depth Hypothesis on phytoplankton blooms. *Ecology*, 91(4), 977–989.

Behrenfeld, M. J., and Boss, E. S. (2014). Resurrecting the Ecological Underpinnings of Ocean Plankton Blooms. *Annual Review of Marine Science*, 6(1), 167–194.

Brainerd, K. E. and Gregg, M. C. (1993). Diurnal restratification and turbulence in the oceanic surface mixed layer: 1. Observations. *Journal of Geophysical Research*, 98(C12).

Brainerd, K. E., and Gregg, M. C. (1995). Surface mixed and mixing layer depths. *Deep Sea Research Part I: Oceanographic Research Papers*, 42(9), 1521–1543.

Brereton, A., Siddons, J., and Lewis, D. M. (2018). Large-eddy simulation of subsurface phytoplankton dynamics: an optimum condition for chlorophyll patchiness induced by Langmuir circulations. *Marine Ecology Progress Series*, 593, 15–27.

Brody, S. R., and Lozier, M. S. (2014). Changes in dominant mixing length scales as a driver of subpolar phytoplankton bloom initiation in the North Atlantic. *Geophysical Research Letters*, 41(9), 3197–3203.

Brody, S. R., and Lozier, M. S. (2015). Characterizing upper-ocean mixing and its effect on the spring phytoplankton bloom with in situ data. ICES Journal of Marine Science, 72(6), 1961–1970.

Chiswell, S. M. (2011). Annual cycles and spring blooms in phytoplankton: don’t abandon Sverdrup completely. *Marine Ecology Progress Series*, 443, 39–50.

Chiswell, S. M., Bradford-Grieve, J., Hadfield, M. G., and Kennan, S. C. (2013). Climatology of surface chlorophyll a, autumn-winter and spring blooms in the southwest Pacific Ocean. *Journal of Geophysical Research: Oceans*, 118(2), 1003–1018.

Chiswell, S. M., Calil, P. H. R., and Boyd, P. W. (2015). Spring blooms and annual cycles of phytoplankton: a unified perspective. *Journal of Plankton Research*, 37(3), 500–508.

Craik, A. D. D., and Leibovich, S. (1976). A rational model for Langmuir circulations. *Journal of Fluid Mechanics*, 73(3), 401–426.

Dale, T., Rey, F., and Sarsia, B. H. (1999). Seasonal development of phytoplankton at a high latitude oceanic site. *Taylor & Francis*.

Ebert, U. (2001). Critical Conditions for Phytoplankton Blooms. Bulletin of Mathematical Biology, 63(6), 1095–1124.

Eilertsen, H. C. (1993). Spring blooms and stratification. *Nature*, 363, 24-24.

Enriquez, R. M., and Taylor, J. R. (2015). Numerical simulations of the competition between wind-driven mixing and surface heating in triggering spring phytoplankton blooms. *ICES Journal of Marine Science*, 72(6), 1926–1941.

Ferrari, R., Merrifield, S. T., and Taylor, J. R. (2015). Shutdown of convection triggers increase of surface cholorophyll. *Journal of Marince Systems*, 147, 116-122.

Fischer, A., Moberg, E., Alexander, H., Brownlee, E., Hunter-Cevera, K., Pitz, K., et al. (2014). Sixty Years of Sverdrup: A Retrospective of Progress in the Study of Phytoplankton Blooms. *Oceanography Society*, 27(1), 222–235.

Franks, P. J. S. (2014). Has Sverdrup's critical depth hypothesis been tested? Mixed layers vs. turbulent layers. *ICES Journal of Marine Science*, 72(6), 1897–1907.

Goh, G., and Noh, Y. (2013). Influence of the Coriolis force on the formation of a seasonal thermocline. *Ocean Dynamics*, 63(9-10), 1083–1092.

Grabowski, W., Dziekan, P., Pawlowska, H. (2018). Lagrangian condensation microphysics with Twomey CCN activation. *Geosci. Model Dev*., 11, 103-120.

Huisman, J., van Oostveen, P., and Weissing, F. J. (1999). Critical depth and critical turbulence: Two different mechanisms for the development of phytoplankton blooms. *Limnology and Oceanography*, 44(7), 1781–1787.

Jokulsdottir, T., and Archer, D. (2016). A stochastic, Lagrangian model of sinking biogenic aggregates in the ocean (SLAMS 1.0): model formulation, validation and sensitivity. *Geoscientific Model Development Discussions*, 9(4), 1455–1476.

Kamykowski, D., Yamazaki, H., and Janowitz, G. S. (1994). A Lagrangian model of phytoplankton photosynthetic response in the upper mixed layer. *Journal of Plankton Research*, 16(8), 1059–1069.

Kida, S., and Ito, T. (2017). A Lagrangian View of Spring Phytoplankton Blooms. *Journal of Geophysical Research: Oceans*, 122(11), 9160–9175.

Kukulka, T., and Brunner, K. (2015). Passive buoyant tracers in the ocean surface boundary layer: 1. Influence of equilibrium wind-waves on vertical distributions. *Journal of Geophysical Research: Oceans*, 120(5), 3837–3858.

Lee, E., Noh, Y., Qiu, B., and Yeh, S.-W. (2015). Seasonal variation of the upper ocean responding to surface heating in the North Pacific. *Journal of Geophysical Research: Oceans*, 120(8), 5631–5647.

Lewis, D. M. (2005). A simple model of plankton population dynamics coupled with a LES of the surface mixed layer. *Journal of Theoretical Biology*, 234(4), 565–591.

Mahadevan, A., D'Asaro, E., Lee, C., and Perry, M. J. (2012). Eddy-Driven Stratification Initiates North Atlantic Spring Phytoplankton Blooms. *Science*, 337(6090), 54–58.

Maronga, B., Gryschka, M., Heinze, R., Hoffmann, F., Kanani- Sühring, F., Keck, M., et al. (2015). The Parallelized Large-Eddy Simulation Model (PALM) version 4.0 for atmospheric and oceanic flows: model formulation, recent developments, and future perspectives. *Geoscientific Model Development Discussions*, 8(8), 2515–2551.

Noh, Y., Min, H. S., and Raasch, S. (2004). Large Eddy Simulation of the Ocean Mixed Layer: The Effects of Wave Breaking and Langmuir Circulation. *Journal of Physical Oceanography*, 34(4), 720–735.

Noh, Y., Kang, I. S., Herold, M., and Raasch, S. (2006). Large eddy simulation of particle settling in the ocean mixed layer. *Physics of Fluids*, 18(8), 085109–16.

Noh, Y., and Lee, W.-S. (2008). Mixed and mixing layer depths simulated by an OGCM. *Journal of Oceanography*, 64(2), 217–225.

Noh, Y., Goh, G., Raasch, S., and Gryschka, M. (2009). Formation of a Diurnal Thermocline in the Ocean Mixed Layer Simulated by LES. *Journal of Physical Oceanography*, 39(5), 1244–1257.

Noh, Y., and Nakada, S. (2010). Estimation of the particle flux from the convective mixed layer by large eddy simulation. *Journal of Geophysical Research*, 115(C5), 1–7.

Noh, Y., Goh, G., and Raasch, S. (2011). Influence of Langmuir Circulation on the Deepening of the Wind-Mixed Layer. *Journal of Physical Oceanography*, 41(3), 472–484.

Obata, A., Ishizaka, J., and Endoh, M. (1996). Global verification of critical depth theory for phytoplankton bloom with climatological in situ temperature and satellite ocean color data. *Journal of Geophysical Research: Atmospheres*, 101(C9), 20657–20667.

Polton, J. A., Smith, J. A., MacKinnon, J. A., and Tejada-Martínez, A. E. (2008). Rapid generation of high-frequency internal waves beneath a wind and wave forced oceanic surface mixed layer. *Geophysical Research Letters*, 35(13), C134–5.

Siegel, D. A. (2002). The North Atlantic Spring Phytoplankton Bloom and Sverdrup's Critical Depth Hypothesis. *Science*, 296(5568), 730–733.

Sullivan, P. P., and McWilliams, J. C. (2010). Dynamics of Winds and Currents Coupled to Surface Waves. *Annual Review of Fluid Mechanics*, 42(1), 19–42.

Sutherland, G., Reverdin, G., Marié, L., and Ward, B., (2014). Mixed and mixing layer depths in the ocean surface boundary layer under conditions of diurnal stratification. *Geophysical Research Letters*, 41, 8419-8476, doi:10.1002/2014GL061939.

Sverdrup, H. U. (1953). On conditions for the vernal blooming of phytoplankton. *ICES Journal of Marine Science*, *18*(3), 287–295.

Taylor, J. R., and Ferrari, R. (2011). Shutdown of turbulent convection as a new criterion for the onset of spring phytoplankton blooms. *Limnology and Oceanography*, *56*(6), 2293–2307.

Taylor, J. R. (2016). Turbulent mixing, restratification, and phytoplankton growth at a submesoscale eddy. *Geophysical Research Letter*, 43, 5784-5792, doi:10.1002/2016GL069016.

Taylor, A. H., and Stephens, J. A. (1993). Diurnal variations of convective mixing and the spring bloom of phytoplankton. *Deep Sea Research Part II: Topical Studies in Oceanography*, *40*(1-2), 389–408.

Townsend, D. W., Cammen, L. M., Holligan, P. M., Campbell, D. E., and Pettigrew, N. R. (1994). Causes and consequences of variability in the timing of spring phytoplankton blooms. *Deep Sea Research Part I: Oceanographic Research Papers*, *41*(5-6), 747–765.

Whitt, D. B., Lévy, M., and Taylor, J. R. (2019). Submesoscales enhance storm driven vertical mixing of nutrients: insights from a biogeochemical large eddy simulation. *Journal of Geophysical Research: Oceans*, *124*(11), 8140-8165.

Woods, J. D., and Onken, R. (1982). Diurnal variation and primary production in the ocean preliminary results of a Lagrangian ensemble model. *Journal of Plankton Research*, *4*(3), 735–756.

Yoshikawa, Y. (2015). Scaling Surface Mixing/Mixed Layer Depth under Stabilizing Buoyancy Flux. *Journal of Physical Oceanography*, *45*(1), 247–258.